Radiology

ORIGINAL RESEARCH • NEURORADIOLOGY

Static Magnetic Fields Dampen Focused Ultrasound–mediated Blood-Brain Barrier Opening

*Yaoheng Yang, MPhil** • *Christopher Pham Pacia, BSc** • *Dezhuang Ye, PhD* • *Yimei Yue, BSc* • *Chih-Yen Chien, MSc* • *Hong Chen, PhD*

From the Departments of Biomedical Engineering (Y. Yang, C.P.P., D.Y., Y. Yue, C.Y.C., H.C.) and Radiation Oncology (H.C.), Washington University in St Louis, 4511 Forest Park Ave, St Louis, MO 63108. Received December 1, 2020; revision requested February 1, 2021; revision received April 6; accepted April 27. **Address correspondence to** H.C. (e-mail: *hongchen@wustl.edu*).

Supported by the National Institutes of Health (R01EB027223, R01EB030102, R01MH116981).

* Y. Yang and C.P.P. contributed equally to this work.

Conflicts of interest are listed at the end of this article.

Radiology 2021; 300:681–689 • https://doi.org/10.1148/radiol.2021204441 • Content code: NR

Background: Focused ultrasound combined with microbubbles has been used in clinical studies for blood-brain barrier (BBB) opening in conjunction with MRI. However, the impact of the static magnetic field generated by an MRI scanner on the BBB opening outcome has not been evaluated.

Purpose: To determine the relationship of the static magnetic field of an MRI scanner on focused ultrasound combined with microbubble-induced BBB opening.

Materials and Methods: Thirty wild-type mice were divided into four groups. Mice from different groups were sonicated with focused ultrasound in different static magnetic fields (approximately 0, 1.5, 3.0, and 4.7 T), with all other experimental parameters kept the same. Focused ultrasound sonication was performed after intravenous injection of microbubbles. Microbubble cavitation activity, the fundamental physical mechanism underlying focused ultrasound BBB opening, was monitored with passive cavitation detection. After sonication, contrast-enhanced T1-weighted MRI was performed to assess BBB opening outcome. Intravenously injected Evans blue was used as a model agent to evaluate trans-BBB delivery efficiency.

Results: The microbubble cavitation dose decreased by an average of 2.1 dB at 1.5 T ($P = .05$), 2.9 dB at 3.0 T ($P = .01$), and 3.0 dB at 4.7 T ($P = .01$) compared with that outside the magnetic field (approximately 0 T). The static magnetic field of an MRI scanner decreased BBB opening volume in mice by 3.2-fold at 1.5 T ($P < .001$), 4.5-fold at 3.0 T ($P < .001$), and 11.6-fold at 4.7 T ($P < .001$) compared with mice treated outside the magnetic field. It also decreased Evans blue trans-BBB delivery 1.4-fold at 1.5 T ($P = .009$), 1.6-fold at 3.0 T ($P < .001$), and 1.9-fold at 4.7 T ($P < .001$).

Conclusion: Static magnetic fields dampened microbubble cavitation activity and decreased trans–blood-brain barrier (BBB) delivery by focused ultrasound combined with microbubble-induced BBB opening.

An earlier incorrect version of this article appeared online. This article was corrected on July 8, 2021.

Increasing numbers of clinical studies have demonstrated the feasibility and safety of focused ultrasound combined with microbubble-mediated blood-brain barrier (BBB) opening in patients with various brain diseases, including Alzheimer disease, glioblastoma, amyotrophic lateral sclerosis, and Parkinson disease (1–7). Most of the reported clinical studies used an MR-guided focused ultrasound system (1–6). MRI is needed for treatment planning, focused ultrasound targeting validation, BBB permeability assessment, and posttreatment safety evaluation (8–10). Clinical studies using neuronavigation-guided focused ultrasound systems (7) or implantable ultrasound devices (11) to perform BBB opening outside an MRI scanner also are ongoing. Safe and effective focused ultrasound BBB opening relies on understanding the impact of all critical parameters on the treatment outcome. Extensive preclinical studies have been performed to assess the dependency of the treatment outcome on various focused ultrasound parameters (12–15), microbubble parameters (16–18), and other treatment protocols (19); however, no study has been performed to evaluate the impact of the magnetic field generated by an MRI scanner.

Microbubble cavitation (ie, the expansion, contraction, and collapse of bubbles in an acoustic field) driven by ultrasound is the fundamental physical mechanism underlying focused ultrasound BBB opening. Since the 1990s, the magnetic field effect has been investigated to understand how cavitation-mediated sonoluminescence was affected by the magnetic field (20). It was reported that bubble dynamics were affected by the magnetic field because moving water molecules around a cavitating bubble interact with the magnetic field by the Lorentz force acting on their electrical-dipole moment, which results in the transformation of kinetic energy into heat (20,21). The magnetic field can be viewed as if the ambient pressure is increased. A theoretical model was developed by modifying the Rayleigh-Plesset equation to incorporate the effect of the magnetic field on bubble oscillation (21). The modified Rayleigh-Plesset equation supports the idea that the magnetic field dampens bubble growth, oscillation, and collapse, and this damping effect increases as the magnetic field strength increases (21,22). Despite advances in experimental and numerical studies of bubble physics, there is a lack of understanding of

Abbreviations

BBB = blood-brain barrier, PCD = passive cavitation detection, ROI = region of interest

Summary

The static magnetic field of an MRI scanner was found to dampen microbubble cavitation activity and decrease the focused ultrasound combined with microbubble-mediated blood-brain barrier opening.

Key Results

- In a murine model study of MRI-guided focused ultrasound combined with microbubble-induced blood-brain barrier (BBB) opening at MRI field strengths ranging from approximately 0 T (outside the magnetic field) to 4.7 T, the static magnetic field dampened the detected microbubble cavitation signal by 2.1 dB at 1.5 T (P = .05), 2.9 dB at 3.0 T (P = .01), and 3.0 dB at 4.7 T (P = .01) compared with that outside the magnetic field.
- The static magnetic field decreased the trans-BBB delivery by focused ultrasound BBB opening by 1.4-fold at 1.5 T (P = .009), 1.6-fold at 3.0 T ($P < .001$), and 1.9-fold at 4.7 T ($P < .001$) compared with that outside the magnetic field.

the effect of the static magnetic field generated by an MRI scanner on microbubble cavitation and the consequent focused ultrasound BBB opening outcome.

We hypothesized that the static magnetic field of an MRI scanner dampens the microbubble cavitation in the focused ultrasound field and reduces focused ultrasound BBB opening. The purpose of this study was to evaluate the impact of the static magnetic field on microbubble cavitation and the associated focused ultrasound BBB opening outcomes.

Materials and Methods

Animal Preparation

All animal studies were reviewed and approved by the institutional animal care and use committee of Washington University in St Louis in accordance with the National Institutes of Health Guidelines for Animal Research (animal protocol number: 20180185). Thirty-two female BALB/c mice aged 8–10 weeks (Charles River Laboratory) were used in this study. Mice were anesthetized with vaporized isoflurane (approximately 1.5%) mixed with oxygen throughout the experiment, and the isoflurane level was kept consistent for all mice. Their body temperature was monitored and maintained at approximately 37°C by blowing warm air. The respiration rate was monitored by using a respiratory pillow sensor and maintained between 50–80 breaths per minute. The fur on each mouse head was removed with a depilatory cream (Nair; Church & Dwight). A catheter was placed in the mouse tail vein for intravenous injection. Two mice were excluded from the study because of failed tail vein injection.

Experimental Setup

An MR-guided focused ultrasound system (Image Guided Therapy) was used. A schematic diagram of the experimental system is shown in Figure 1A. The system consisted of an MRI-compatible focused ultrasound transducer (Imasonics) made of a seven-element annular array with a center frequency of 1.5 MHz, an aperture of 25 mm, and a radius of curvature of 20 mm. The annular array design of the focused ultrasound transducer allowed it to electronically steer the focus in the axial direction (z-axis). The transducer was connected to an MRI-compatible piezoelectric motor, allowing the position of the transducer to be mechanically adjusted in the lateral directions (along the x- and y-axes). The output of the focused ultrasound transducer was calibrated using a piezoelectric hydrophone (HGL-0200; Onda) outside the MRI scanner. The axial and lateral full width at half maximums of the focused ultrasound transducer were 5.5 mm and 1.2 mm, respectively. The acoustic pressure reported in this study was corrected for 18% mouse skull attenuation (23). The passive cavitation detection (PCD) sensor at the center of the focused ultrasound transducer had a center frequency of 1.6 MHz and a –6-dB bandwidth of 754 kHz. The signals detected with the PCD sensor were acquired via the PicoScope (5000 series; Pico Technology). The transducer set (focused ultrasound and PCD) was connected to a water balloon filled with deionized and degassed water and coupled to the mouse head with degassed ultrasound gel. To avoid the interference of the fringe field, the radiofrequency generator, Picoscope, and personal computer were positioned well outside the fringe magnetic field of the MRI scanner (approximately 0 T) (Fig 1A).

Focused Ultrasound Treatment

Mice were randomly assigned to four groups. Each group was treated at different distances from the isocenter of an unshielded 4.7-T MRI scanner (Fig 1A). The static magnetic field at each location was 4.7, 3.0, 1.5, and approximately 0 T (outside of the 0.0005-T line, which is approximately 3.0 m along the magnetic axis) using a gaussmeter (RoHS; FW Bell). All four groups of mice were treated by following the same experimental procedure using the same microbubble and focused ultrasound parameters, with the only difference being the static magnetic fields. Focused ultrasound treatment was performed by two authors (C.P.P. and D.Y., with 3 and 5 years of experience, respectively). The focused ultrasound planning was performed with the guidance of a 4.7-T small-animal MRI scanner (Agilent/Varian DirectDriveTM console; Agilent Technologies) using the MR-guided focused ultrasound software (ThermoGuide; Image Guided Therapy) to target the focused ultrasound transducer at the left side of the cerebellum and brainstem (24). A gadolinium-based MR contrast agent, gadoterate meglumine (Dotarem; 0.05 mmol/mL, 50 μl per mouse) was co-injected with microbubbles (200 μL per kilogram of body weight; Definity; Lantheus Medical Imaging) through the tail vein catheter followed by focused ultrasound sonication (center frequency, 1.5 MHz; peak negative pressure, 0.6 MPa; duty cycle, 3.33%; burst length, 6.66 msec; pulse repetition frequency, 5 Hz; and sonication duration, 1 minute).

To ensure that the acoustic output of the focused ultrasound system was not affected by the static magnetic field, the acoustic pressure at the focus of the focused ultrasound transducer in

different magnetic fields was examined with an MRI-compatible fiber-optic hydrophone (HFO-690; Onda) using a method similar to that used in our previous publications (25–27). The fiber-optic hydrophone was placed in a container that was positioned in front of the focused ultrasound transducer. The tip of the optical fiber was located at the focus of the focused ultrasound transducer. Measurements of transducer output were performed by placing the transducer at different distances from the isocenter of the 4.7-T MRI scanner. The distances were kept the same as in the animal experiment (Fig 1A). The fiber-optic hydrophone had low sensitivity; therefore, more than 1000 repeatedly acquired signals were averaged for each measurement to increase the signal-to-noise ratio. The mean peak negative pressure and peak positive pressure measured in each magnetic field strength were calculated from three repeated measurements. There was no significant difference in the measured peak negative and positive pressures for different magnetic fields (Fig 1C–1E), which enabled us to confirm that the acoustic output of the focused ultrasound transducer was not influenced by the static magnetic field.

Microbubble Cavitation Activity Detection and Quantification

Before microbubble injection, PCD signals were recorded for 60 seconds and were used to define the baselines for cavitation quantification. To ensure that the recorded PCD signals were not affected by the static magnetic field, the PCD baseline signals acquired in different static magnetic fields (approximately 0, 1.5, 3.0, and 4.7 T) were compared. The mean and standard deviation of the peak positive and peak negative voltages of the PCD baseline signals were calculated for mice sonicated in each magnetic field. The peak positive and negative voltages of the PCD baseline signals were not significantly different for various magnetic fields (Fig 1F–1H), indicating that the PCD signal acquisition system was not influenced by the static magnetic field.

PCD was used to detect the acoustic emissions from microbubbles during focused ultrasound sonication. The acquired PCD signals were processed using an established method to quantify the stable and inertial cavitation doses, which were used to assess the amount of energy associated with these two types of cavitation activity (28). A fast-Fourier transform was performed for each signal acquired during the sonication of each focused ultrasound pulse. The stable cavitation level was calculated as the root mean squared amplitude of the subharmonic ($1/2f_0$; f_0: center frequency of the focused ultrasound transducer) and second ($2f_0$) and third ($3f_0$) harmonic signals within 3-kHz bandwidths. The inertial cavitation level was calculated by the root mean squared amplitude of the frequency spectrum after excluding 300-kHz bandwidths around all the harmonics (nf_0, where n = 1, 2, 3) and ultraharmonics ($mf_0/2$, where m = 1, 3, 5, 7) signals. The stable and inertial cavitation levels calculated based on signals acquired during focused ultrasound sonication after microbubble injection were normalized by the corresponding levels and calculated using signals acquired before microbubble injection. The stable cavitation dose was quantified by the cumulative sum of the stable cavitation levels calculated for the whole focused ultrasound sonication duration and then normalized to the corresponding cavitation dose of the baseline. The stable cavitation dose was then converted to decibel format. Inertial cavitation dose was calculated in the same way based on the inertial cavitation level.

Quantification of BBB Opening with Contrast-enhanced MRI

Approximately 5 minutes after the completion of focused ultrasound sonication (Fig 1B), all mice were imaged using a T1-weighted gradient-echo sequence (repetition time msec/echo time msec, 108/4; section thickness, 0.5 mm; in-plane resolution, 0.25 × 0.25 mm; matrix size, 128 × 128; number of signal averages, 16; flip angle, 60°). As the intravenously injected gadoterate meglumine was too large to cross an intact BBB, the BBB opening outcome was quantified based on hyperenhancement on the T1-weighted images, which indicated the leakage of gadoterate meglumine. The BBB opening volume was quantified by two authors (Y. Yang, with 7 years of experience in MATLAB programming; C.P.P., with 4 years of experience) using a customized MATLAB program (Mathworks). First, two circular regions of interest (ROIs) (2.4 mm in diameter, double the full width at half maximum of the focused ultrasound focal size in the horizontal plane) were drawn in the focused ultrasound–treated site and the contralateral untreated site, respectively. Second, a voxel within the focused ultrasound–treated ROI was considered to represent the BBB opening if the voxel intensity was more than three standard deviations above the mean intensity of the nontreated ROI. Third, the total volume of the voxels representing the BBB opening was calculated by the summation of those voxels identified in all brain sections along the focused ultrasound beam path. The percentage of normalized signal intensity change was calculated by the mean signal intensity increase in the focused ultrasound–treated ROI compared with the untreated ROI and normalized to the mean signal intensity in the untreated ROI.

Quantification of Evans Blue Extravasation

Evans blue (4%, 60 μL) was injected intravenously into the mice about 20 minutes after sonication (Fig 1B). Evans blue was used as a model drug to evaluate whether the magnetic field affects trans-BBB drug delivery efficiency. Two hours after injection of Evans blue, all mice underwent transcardial perfusion using phosphate-buffered saline (0.01 mol/L, 30 mL) followed by paraformaldehyde (4%, 30 mL) under anesthesia. The mouse brains were extracted after perfusion. The brains were imaged with the Pearl small animal imaging system (LI-COR Biosciences) using the 700-nm channel with the same exposure settings for all mice. The fluorescence intensity of the brains was then quantified using Image Studio Lite software (LI-COR Biosciences) by one author (Y. Yang, with 1 year of experience). ROIs (2.4 mm in diameter) centered at the location with the maximum fluorescence signal were drawn using the software. The total optical density within the ROIs was calculated and normalized to that calculated based on ROIs selected in the untreated site (12,29). After fluorescence imaging, the mouse brains were fixed in 4% paraformaldehyde

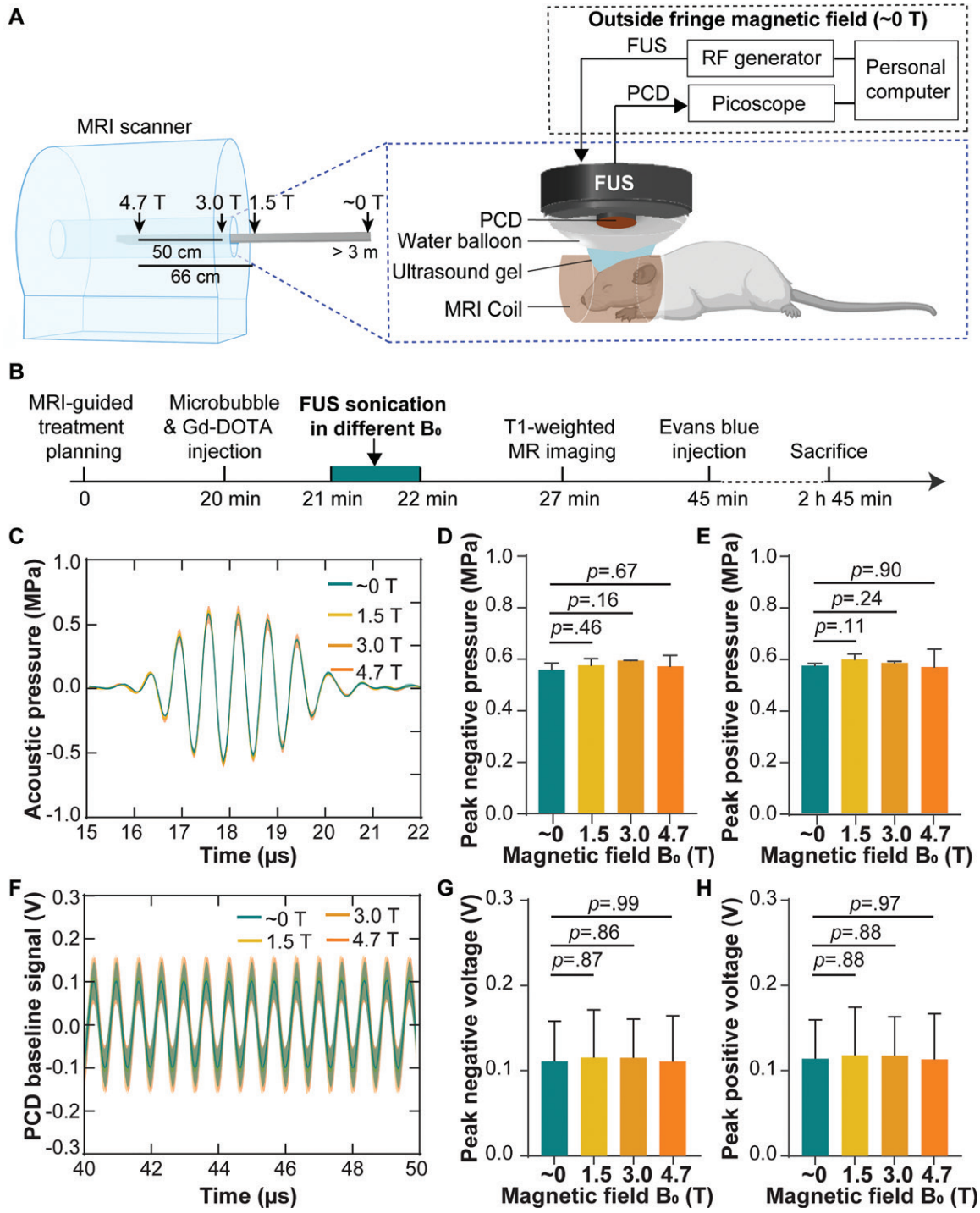

Figure 1: **(A)** Illustration of the experimental setup. Focused ultrasound (FUS) sonication was performed in different static magnetic fields (approximately 0, 1.5, 3.0, and 4.7 T) by positioning the mice at different distances from the isocenter of the MRI scanner. **(B)** Experimental timeline. **(C)** Acoustic pressure waveforms at the focus of the focused ultrasound transducer measured with an MRI-compatible fiber-optic hydrophone in different magnetic fields. Each solid line and shadow represents the mean ± standard deviation, respectively, of three repeated measurements in each magnetic field. Comparisons of **(D)** the peak negative pressure and **(E)** peak positive pressure in different magnetic fields. **(F)** Passive cavitation detection (PCD) baseline signals received when focused ultrasound was on but without microbubbles in different magnetic fields. The phase delays of the PCD baseline signals acquired from different mice in each magnetic field were calculated by means of cross correlation and compensated for calculating the mean (solid line) and standard deviation (shadow) of these signals. Comparisons of **(G)**, the peak negative voltage and **(H)** peak positive voltage of the PCD baseline signals in different magnetic fields. Error bars indicate standard deviation. Gd-DOTA = gadoterate meglumine, RF = radiofrequency.

for 24 hours. The mouse brains were then cryoprotected by sucrose and cut into 15-μm-thick slices along the horizontal plane to be stained with hematoxylin-eosin to evaluate the safety of the treatment (Y. Yue, with 10 years of experience).

Statistical Analysis

Statistical analysis was performed by using GraphPad Prism (version 8.3; GraphPad) software by one author (Y. Yang, with 6 years of experience). A two-tailed unpaired *t* test was used for comparison of the groups treated in different static magnetic fields (1.5 T, 3.0 T, and 4.7 T) with the group treated outside the static magnetic field (approximately 0 T).

Results

Magnetic Fields Dampened Microbubble Cavitation Activity

The hallmarks of stable cavitation, including subharmonic ($1/2f_0$; f_0: center frequency of the focused ultrasound transducer) and second ($2f_0$), and third ($3f_0$) harmonic signals, showed a trend of decreasing amplitude as the magnetic field strength increased (Fig 2A). The amplitude of the stable cavitation level over the whole course of focused ultrasound treatment (60 seconds) decreased when comparing mice treated outside the MRI scanner magnetic field (approximately 0 T) with those treated inside the MRI scanner magnetic field at 1.5 T, 3.0 T, and 4.7 T (Fig 2B). The mean stable cavitation dose, as the cumulated stable cavitation level over sonication duration, was 4.4 dB ± 0.8 (standard error of the mean) for the group treated outside the magnetic field of the MRI scanner (approximately 0 T). In contrast, it significantly and monotonically decreased to a mean of 2.3 dB ± 0.6 at 1.5 T, 1.5 dB ± 0.4 at 3.0 T, and 1.4 dB ± 0.5 at 4.7 T, corresponding to decreases by an average of 2.1 dB at 1.5 T (P = .05), 2.9 dB at 3.0 T (P = .01), and 3.0 dB at 4.7 T (P = .01) compared with that outside the magnetic field (approximately 0 T) (Fig 2C). Because the acoustic pressure used in this study was low, inertial cavitation was not detected (Fig 2B, 2C).

Static Magnetic Fields Decreased BBB Opening

Focused ultrasound treatment performed in different magnetic fields showed localized BBB opening, as indicated by the bright spots on contrast-enhanced MRI scans (Fig 3A). The region with hyperenhancement was confined to the focused ultrasound–targeted brain location and was not observed in the contralateral untreated area, demonstrating the capability of focused ultrasound to achieve a spatially localized BBB opening. However, mice treated inside the magnetic field with a different magnetic field (1.5 T, 3.0 T, or 4.7 T) had lower contrast enhancement within a smaller region than those treated outside the magnetic field (approximately 0 T). The mean BBB opening volume obtained outside the magnetic field (approximately 0 T) was 5.8 mm^3 ± 0.6 and significantly and monotonically decreased to 1.8 mm^3 ± 0.3 at 1.5 T, 1.3 mm^3 ± 0.3 at 3.0 T, and 0.5 mm^3 ± 0.1 at 4.7 T, corresponding to decreases by 3.2-fold at 1.5 T (P < .001), 4.5-fold at 3.0 T (P < .001), and 11.6-fold at 4.7 T (P < .001) compared with the volume at approximately 0 T (Fig 3B). The focused ultrasound–BBB opening induced 84.1% signal intensity change at the target location when the mice were treated outside the magnetic field (approximately 0 T), while this value decreased to 49.1% at 1.5 T, 35.7% at 3.0 T, and 7.1% at 4.7 T (Fig 3C). The signal intensity change was decreased 1.7-fold at 1.5 T (P = .05), 2.4-fold at 3.0 T (P = .007), and 11.8-fold at 4.7 T (P < .001) compared with that outside the magnetic field (approximately 0 T).

Static Magnetic Fields Reduced Evans Blue Delivery

The fluorescence images of the ex vivo mouse brains showed that the fluorescence intensity of the Evans blue was significantly lower in mice sonicated at 1.5 T, 3.0 T, or 4.7 T compared with mice treated outside the magnetic field (approximately 0 T) (Fig 4A). The Evans blue fluorescence intensity was 217.9 ± 8.3 at approximately 0 T, 161.0 ± 16.6 at 1.5 T, 135.8 ± 15.5 at 3.0 T, and 117.6 ± 18.1 at 4.7 T (Fig 4B). The Evans blue trans-BBB delivery was decreased by 1.4-fold at 1.5 T (P = .009), 1.6-fold at 3.0 T (P < .001), and 1.9-fold at 4.7 T (P < .001) when compared with that at approximately 0 T.

Safety of Focused Ultrasound Treatment

No evident hemorrhage or tissue damage was observed in mice treated outside or inside the MRI scanner. As shown by the representative images of the hematoxylin-eosin–stained brain slice (Fig 5), neither red blood cell extravasation nor cellular nuclei loss was observed at the focused ultrasound–targeted brain location (Fig 5).

Discussion

Recent success in multiple early-phase clinical trials has demonstrated the great promise of focused ultrasound combined with microbubble-induced blood-brain barrier (BBB) opening in the treatment of various brain diseases, and MRI is often used for real-time guidance of the procedure (1–6). Extensive preclinical studies have been reported in the past 2 decades to evaluate the dependency of the treatment outcome on various parameters; however, the impact of the static magnetic field generated by an MRI scanner on the BBB opening outcome has been overlooked. The present study revealed that the static magnetic field dampened the cavitation activity generated by focused ultrasound–activated microbubbles and decreased the BBB opening volume and model drug delivery efficiency.

The magnetic field is known to dampen bubble oscillation in an ultrasound field based on numeric modeling and in vitro sonoluminescence examination (20–22). The current study confirmed that this dampening effect also exists in MR-guided focused ultrasound combined with microbubble-mediated BBB opening in vivo in clinically relevant magnetic field strengths. When compared with focused ultrasound treatment outside the MRI scanner, the magnetic field dampened the microbubble cavitation activity, and the dampening effect enhanced with increasing magnetic field in a monotonic manner. This finding agreed with findings of previous theoretical and experimental studies reporting that the magnetic field acts against bubble oscillation, and the dampening effect is positively correlated to the magnetic field strength (21,22). The dampening effect of the magnetic field on free bubbles (without shells) is considered to be caused by the loss of bubble kinetic energy due to the Lorentz force acting on the

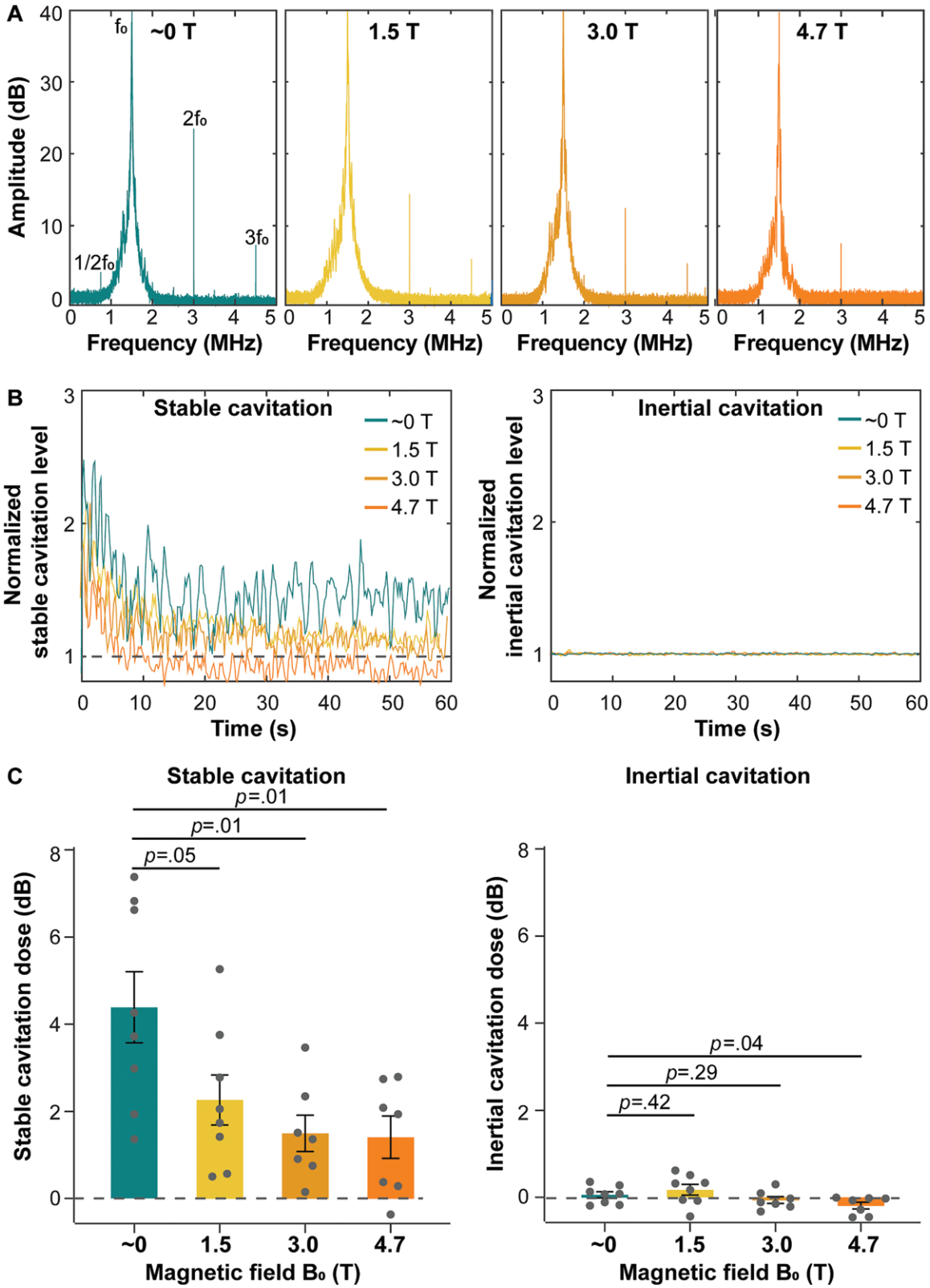

Figure 2: Cavitation activities in vivo during focused ultrasound sonication in different static magnetic fields. **(A)** Representative spectrums of passive cavitation detection (PCD) signals acquired during focused ultrasound sonication in approximately 0, 1.5, 3.0, and 4.7 T. f_0 = fundamental frequency of focused ultrasound. **(B)** Representative plots of normalized stable cavitation level (left) and inertial cavitation level (right) as a function of time for mice treated in different magnetic fields. **(C)** Stable cavitation doses (left) and inertial cavitation doses (right) of mice sonicated in different magnetic fields. Each dot represents a measurement from one mouse. Error bars indicate standard error of the mean.

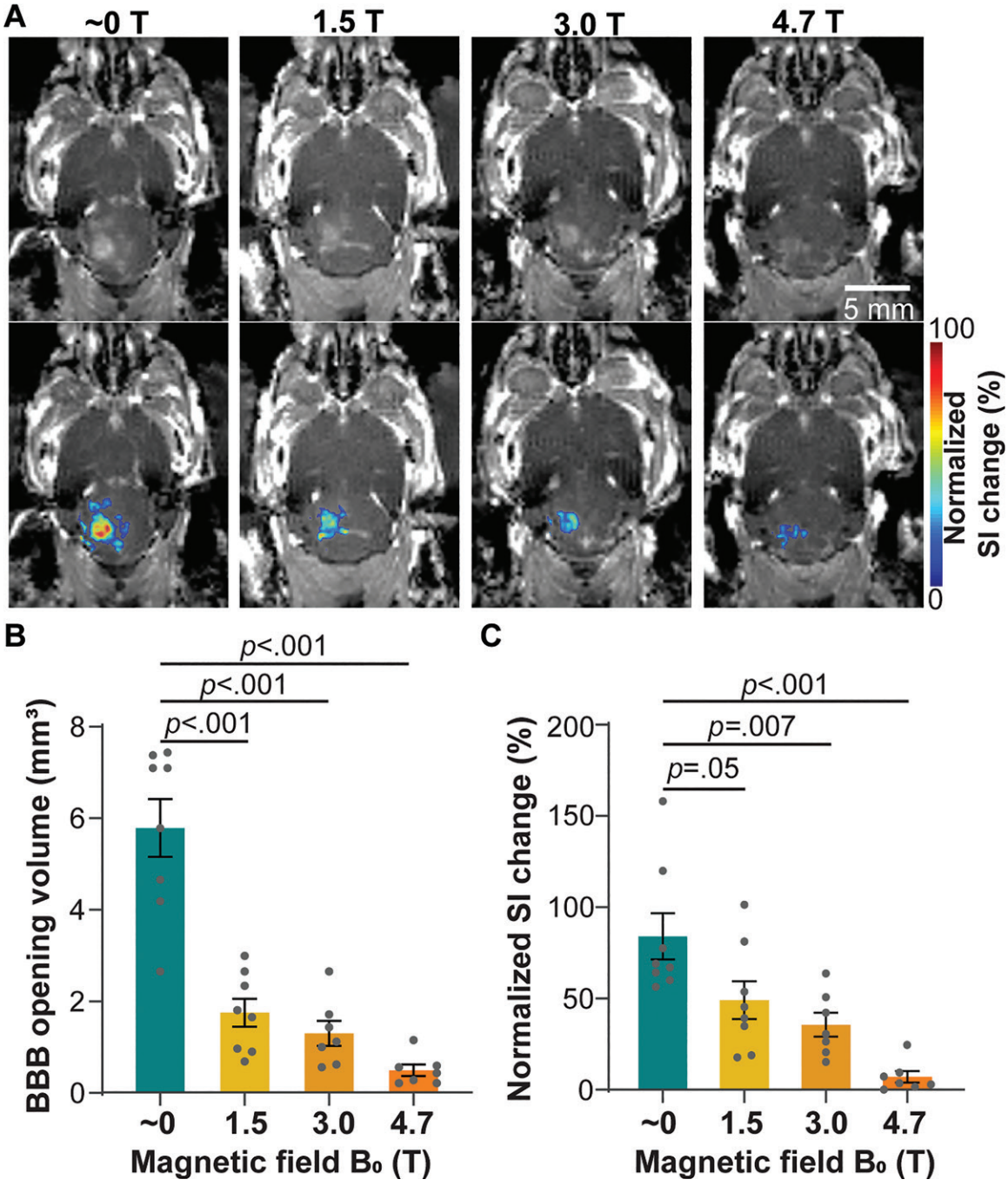

Figure 3: Contrast-enhanced MRI of mice treated with focused ultrasound–induced blood-brain barrier (BBB) opening in different magnetic fields. **(A)** Representative contrast-enhanced T1-weighted horizontal MRI scans show BBB opening in mice sonicated in different magnetic fields (approximately 0, 1.5, 3.0, and 4.7 T; top panel). BBB opening area is superimposed on the T1-weighted MRI scan, with the color indicating the normalized signal intensity (SI) change (bottom panel). **(B)** Quantification of the BBB opening volume of mice treated in different magnetic fields. **(C)** Quantification of normalized signal intensity change at the focused ultrasound–targeted location, comparing mice treated in different magnetic fields. Error bars indicate standard error of the mean.

moving dipolar water molecules (21). The lipid shell of Definity microbubbles carries negative charges (30). It is likely that moving charged lipid molecules on the microbubble shell during cavitation may generate additional Lorentz force that also contributes to the observed dampening effect of the magnetic field on microbubble cavitation. The dampened microbubble oscillation is expected to generate lower mechanical forces on the vessel wall, leading to decreased BBB opening volume and lower drug delivery efficiency. Indeed, findings from the current study showed a clear trend that increasing magnetic field led to decreases in the BBB opening volume and trans-BBB delivery efficiency.

There are a growing number of clinical trials on evaluating focused ultrasound combined with microbubble-induced BBB opening in patients with various diseases. Most clinical

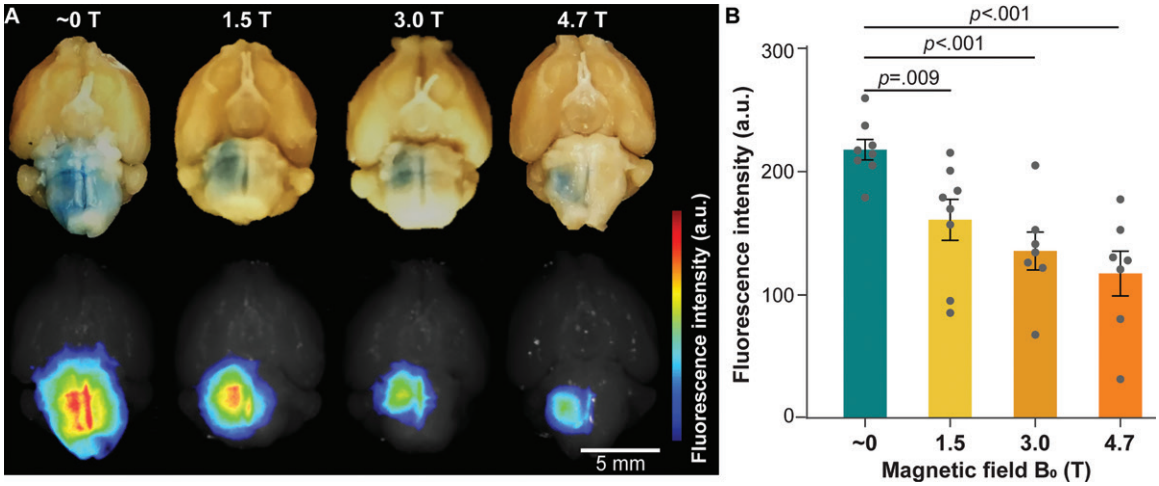

Figure 4: Evans blue delivery via focused ultrasound combined with microbubble-induced blood-brain barrier opening in different magnetic fields. **(A)** Representative photographs (top row) and corresponding fluorescence images (bottom row) of mouse brains treated in magnetic fields of approximately 0 T, 1.5 T, 3.0 T, and 4.7 T. **(B)** Fluorescence intensity quantification of mice treated in magnetic fields of approximately 0 T, 1.5 T, 3.0 T, and 4.7 T. Error bars indicate standard error of the mean.

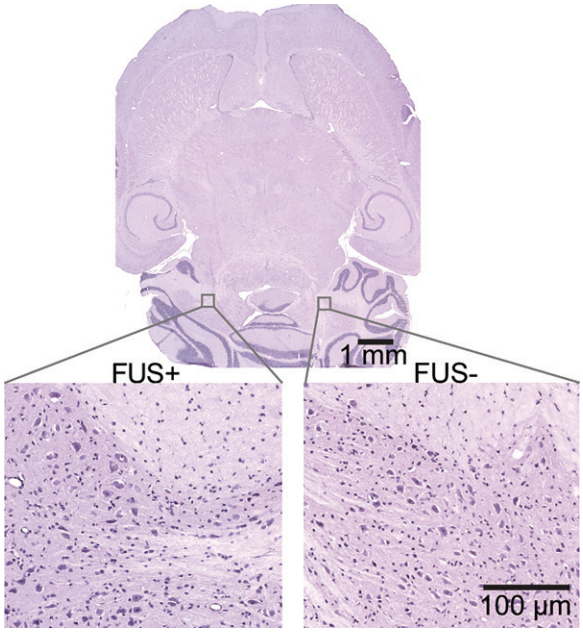

Figure 5: Hemotoxylin-eosin–stained horizontal whole-brain slice (top panel) with higher-magnification images (bottom panels) obtained from the focused ultrasound–treated brain region (FUS+) and contralateral untreated control region (FUS–). No gross tissue damage was observed on the whole-brain slice. Higher-magnification images showed that erythrocyte extravasation and neuronal damage were not observed in either the focused ultrasound–treated brain region or the untreated control brain region.

trials use clinical 3.0-T MRI scanners coupled with the InSightec focused ultrasound system (InSightec). However, there also are clinical trials that use implantable ultrasound devices and neuronavigational-guided focused ultrasound. Our present study found that the 3.0-T magnetic field dampened the cavitation dose by approximately 2.9 dB, decreased the BBB opening volume by 4.5-fold, and reduced Evans blue delivery efficiency by 1.6-fold compared with values obtained outside the magnetic field (approximately 0 T). These findings suggest that it is crucial to consider the impact of the magnetic field when designing a study or comparing results obtained with different ultrasound systems. In addition to brain drug delivery, cavitation is also the fundamental physical mechanism for several other therapeutic techniques, such as histotripsy and sonothrombolysis (31,32). The dampening effect induced by the magnetic field on cavitation is expected to affect the treatment outcomes of other cavitation-mediated techniques when MR-guided focused ultrasound systems are used.

This study had several limitations. First, the magnetic field at 1.5 T and 3.0 T was produced by positioning mice at specific distances along the main axis of a 4.7-T MRI scanner. While the magnetic field homogeneity is imperfect outside of the magnet isocenter, the variations are small over the scale of the mouse head. By positioning the animal different distances away from the isocenter, we were able to perform all experiments using the same focused ultrasound system in the same MRI scanner to ensure all other experimental conditions were kept consistent. Future study is warranted to verify the observed effects by comparing studies performed using different MRI scanners. Second, the present study used the MR contrast agent and the Evans blue as model agents to assess focused ultrasound with microbubble-induced BBB opening outcomes. The impact of the magnetic field on the delivery outcomes of therapeutic agents needs to be examined in the future. Third, we only performed focused ultrasound treatment using one set of focused ultrasound and microbubble parameters. Future studies are needed to investigate the impact of the magnetic field under different focused ultrasound and microbubble parameters to fully characterize the effects of the magnetic field on microbubble cavitation and the consequent BBB opening outcomes. Lastly, PCD measures the acoustic emissions from microbubble cavitation, which provides an indirect measurement of microbubble dynamics. Direct proof of the effect of the static magnetic field on microbubble cavitation can be obtained in the future by using

high-speed photomicrography (33) to directly record the microbubble dynamics in the presence of static magnetic fields.

This study revealed, for the first time, the dampening effect of the magnetic field on focused ultrasound–activated microbubble cavitation activity and cavitation-induced blood-brain barrier opening. Findings from this study suggest that the impact of the magnetic field needs to be considered in the clinical applications of MR-guided focused ultrasound in drug delivery to the brain. Future study is needed to further investigate the impact of the magnetic field on MR-guided focused ultrasound combined with microbubble-mediated therapies.

Acknowledgments: Portions of this work were conducted using the Small Animal Magnetic Resonance Facility of the Mallinckrodt Institute of Radiology, Washington University. We also thank Dr James D. Quirk for helping with the technical issues of the MRI scanner.

Author contributions: Guarantors of integrity of entire study, Y. Yang, C.P.P., D.Y., C.Y.C., H.C.; study concepts/study design or data acquisition or data analysis/interpretation, all authors; manuscript drafting or manuscript revision for important intellectual content, all authors; approval of final version of submitted manuscript, all authors; agrees to ensure any questions related to the work are appropriately resolved, all authors; literature research, Y. Yang, D.Y., H.C.; experimental studies, all authors; statistical analysis, Y. Yang, C.P.P., H.C.; and manuscript editing, Y. Yang, C.P.P., D.Y., H.C.

Disclosures of Conflicts of Interest: **Y .Yang** disclosed no relevant relationships. **C.P.P.** disclosed no relevant relationships. **D.Y.** disclosed no relevant relationships. **D.Y.** disclosed no relevant relationships. **Y. Yue** disclosed no relevant relationships. **C.Y.C.** disclosed no relevant relationships. **H.C.** disclosed no relevant relationships.

References

1. Rezai AR, Ranjan M, D'Haese PF, et al. Noninvasive hippocampal blood-brain barrier opening in Alzheimer's disease with focused ultrasound. Proc Natl Acad Sci U S A 2020;117(17):9180–9182.
2. Abrahao A, Meng Y, Llinas M, et al. First-in-human trial of blood-brain barrier opening in amyotrophic lateral sclerosis using MR-guided focused ultrasound. Nat Commun 2019;10(1):4373.
3. Lipsman N, Meng Y, Bethune AJ, et al. Blood-brain barrier opening in Alzheimer's disease using MR-guided focused ultrasound. Nat Commun 2018;9(1):2336.
4. Meng Y, Abrahao A, Heyn CC, et al. Glymphatics visualization after focused ultrasound-induced blood–brain barrier opening in humans. Ann Neurol 2019;86(6):975–980.
5. Mainprize T, Lipsman N, Huang Y, et al. Blood-brain barrier opening in primary brain tumors with non-invasive MR-guided focused ultrasound: A clinical safety and feasibility study. Sci Rep 2019;9(1):321.
6. D'Haese PF, Ranjan M, Song A, et al. β-Accocampus after focused ultrasound-induced blood–brain barrier opening in Alzheimer's disease. Front Hum Neurosci 2020;14:593672.
7. Chen KT, Lin YJ, Chai WY, et al. Neuronavigation-guided focused ultrasound (NaviFUS) for transcranial blood-brain barrier opening in recurrent glioblastoma patients: clinical trial protocol. Ann Transl Med 2020;8(11):673.
8. McDannold N, Vykhodtseva N, Raymond S, Jolesz FA, Hynynen K. MRI-guided targeted blood-brain barrier disruption with focused ultrasound: histological findings in rabbits. Ultrasound Med Biol 2005;31(11):1527–1537.
9. Liu HL, Hua MY, Yang HW, et al. Magnetic resonance monitoring of focused ultrasound/magnetic nanoparticle targeting delivery of therapeutic agents to the brain. Proc Natl Acad Sci U S A 2010;107(34):15205–15210.
10. Kinoshita M, McDannold N, Jolesz FA, Hynynen K. Noninvasive localized delivery of Herceptin to the mouse brain by MRI-guided focused ultrasound-induced blood-brain barrier disruption. Proc Natl Acad Sci U S A 2006;103(31):11719–11723.
11. Carpentier A, Canney M, Vignot A, et al. Clinical trial of blood-brain barrier disruption by pulsed ultrasound. Sci Transl Med 2016;8(343):343re2.
12. Morse SV, Pouliopoulos AN, Chan TG, et al. Rapid short-pulse ultrasound delivers drugs uniformly across the murine blood-brain barrier with negligible disruption. Radiology 2019;291(2):459–466.
13. McDannold N, Vykhodtseva N, Hynynen K. Blood-brain barrier disruption induced by focused ultrasound and circulating preformed microbubbles appears to be characterized by the mechanical index. Ultrasound Med Biol 2008;34(5):834–840.
14. Kinoshita M, McDannold N, Jolesz FA, Hynynen K. Targeted delivery of antibodies through the blood-brain barrier by MRI-guided focused ultrasound. Biochem Biophys Res Commun 2006;340(4):1085–1090.
15. Kamimura HA, Flament J, Valette J, et al. Feedback control of microbubble cavitation for ultrasound-mediated blood-brain barrier disruption in non-human primates under magnetic resonance guidance. J Cereb Blood Flow Metab 2019;39(7):1191–1203.
16. Song KH, Fan AC, Hinkle JJ, Newman J, Borden MA, Harvey BK. Microbubble gas volume: A unifying dose parameter in blood-brain barrier opening by focused ultrasound. Theranostics 2017;7(1):144–152.
17. McDannold N, Vykhodtseva N, Hynynen K. Use of ultrasound pulses combined with Definity for targeted blood-brain barrier disruption: a feasibility study. Ultrasound Med Biol 2007;33(4):584–590.
18. Choi JJ, Feshitan JA, Baseri B, et al. Microbubble-size dependence of focused ultrasound-induced blood-brain barrier opening in mice in vivo. IEEE Trans Biomed Eng 2010;57(1):145–154.
19. McDannold N, Zhang Y, Vykhodtseva N. Blood-brain barrier disruption and vascular damage induced by ultrasound bursts combined with microbubbles can be influenced by choice of anesthesia protocol. Ultrasound Med Biol 2011;37(8):1259–1270.
20. Young JB, Schmiedel T, Kang W. Sonoluminescence in high magnetic fields. Phys Rev Lett 1996;77(23):4816–4819.
21. Yasui K. Effect of a magnetic field on sonoluminescence. Phys Rev E Stat Phys Plasmas Fluids Relat Interdiscip Topics 1999;60(2 Pt B):1759–1761.
22. Behnia S, Mobadersani F, Yahyavi M, Rezavand A, Hoesinpour N, Ezzat A. Effect of magnetic field on the radial pulsations of a gas bubble in a non-Newtonian fluid. Chaos Solitons Fractals 2015;78:194–204.
23. Choi JJ, Pernot M, Small SA, Konofagou EE. Noninvasive, transcranial and localized opening of the blood-brain barrier using focused ultrasound in mice. Ultrasound Med Biol 2007;33(1):95–104.
24. Ye D, Zhang X, Yue Y, et al. Focused ultrasound combined with microbubble-mediated intranasal delivery of gold nanoclusters to the brain. J Control Release 2018;286:145–153.
25. Zhu L, Nazeri A, Pacia CP, Yue Y, Chen H. Focused ultrasound for safe and effective release of brain tumor biomarkers into the peripheral circulation. PLoS One 2020;15(6):e0234182.
26. Kothapalli SVVN, Partanen A, Zhu L, et al. A convenient, reliable, and fast acoustic pressure field measurement method for magnetic resonance-guided high-intensity focused ultrasound systems with phased array transducers. J Ther Ultrasound 2018;6(1):5.
27. Kothapalli SVVN, Altman MB, Partanen A, et al. Acoustic field characterization of a clinical magnetic resonance-guided high-intensity focused ultrasound system inside the magnet bore. Med Phys 2017;44(9):4890–4899.
28. Chen H, Konofagou EE. The size of blood-brain barrier opening induced by focused ultrasound is dictated by the acoustic pressure. J Cereb Blood Flow Metab 2014;34(7):1197–1204.
29. Choi JJ, Selert K, Vlachos F, Wong A, Konofagou EE. Noninvasive and localized neuronal delivery using short ultrasonic pulses and microbubbles. Proc Natl Acad Sci U S A 2011;108(40):16539–16544.
30. Ja'afar F, Leow CH, Garbin V, Sennoga CA, Tang MX, Seddon JM. Surface charge measurement of sonovue, definity and optison: A comparison of laser doppler electrophoresis and micro-electrophoresis. Ultrasound Med Biol 2015;41(11):2990–3000.
31. Roberts WW, Hall TL, Ives K, Wolf JS Jr, Fowlkes JB, Cain CA. Pulsed cavitational ultrasound: a noninvasive technology for controlled tissue ablation (histotripsy) in the rabbit kidney. J Urol 2006;175(2):734–738.
32. Alexandrov AV, Molina CA, Grotta JC, et al. Ultrasound-enhanced systemic thrombolysis for acute ischemic stroke. N Engl J Med 2004;351(21):2170–2178.
33. Chen H, Kreider W, Brayman AA, Bailey MR, Matula TJ. Blood vessel deformations on microsecond time scales by ultrasonic cavitation. Phys Rev Lett 2011;106(3):034301.